Chapter 2

Electrochemical Synthesis of Monolayer Protected Clusters of Gold

In this chapter, a novel electrochemical method of synthesis of thiol stabilized inorganic gold nanoparticles (Au NPs) is described. The method presented here forms the basis for the nanoparticle immobilization on solid substrates which is described in detail in the next chapter. The electrochemical method has several advantages since the desired amount of nanoparticles can be prepared *in situ* by programming the current and time (charge) with a better control of its size. This will overcome wastage of nanoparticles since they normally tend to agglomerate over a period of time. By electrochemical method, the nanoparticles can also be produced in a localized region by simple passage of current between two electrodes in a suitable medium. The size of the nanocrystals could be tuned by varying different experimental conditions such as reaction time, temperature, and the inter electrode separations.

We have synthesized the thiol stabilized gold nanoparticles (Au NPs), also called monolayer protected clusters of gold (MPCs), for the first time by the process of electrochemical dissolution of gold. The Au NPs can be produced using KCl as a supporting electrolyte both with and without $NaBH_4$ as a reducing agent in the presence of alkanethiols such as decanethiol (DT) or functionalized thiol such as 11-mercaptoundecanoic acid (MUA). The thiol capped Au NPs were characterized by UV-vis absorption, Fourier transform infrared spectroscopy (FTIR) and transmission electron microscopy (TEM) studies.

2.1 Introduction

Colloidal metal nanoparticles, especially noble metal nanoparticles have gained a considerable interest in recent years due to their immense applications in optoelectronics, catalysis, drug delivery, immuno-assay [1-13], and energy conversion as well as in fundamental studies in quantum physics [14-18]. Although, there are numerous methods available for synthesizing nanoparticles, several challenges remain in attaining the desired properties. The method to be used depends strongly on the type of particle to be synthesized, the particles functional medium, and the surface to which they will be attached etc., Many synthetic methods are available to form

colloidal suspensions. The dimensions of these nanoparticles can be tailored as well as their surface functionalities. It is also possible to influence some level of control of their shape. This is achieved through control of the conditions and parameters during synthesis [1, 19]. One of the greatest challenges faced in nanoparticles synthesis is the instability of the nanoparticles and their tendency to easily aggregate or precipitate. These effects are avoided through the use of stabilizing agents that adhere to the surface of the nanoparticles. Generally, these stabilizing agents can manipulate the solubility, growth and surface charge of the particles. As a result, they keep the particles separated and suspended in the liquid environment during their synthesis [20-22]. One of the conventional methods of synthesis of gold nanoparticles is by the reduction of Au (III) derivatives. The traditional approaches to prepare nanoparticles on supports involve co-precipitation, deposition-precipitation, ion-exchange, impregnation, successive reduction and calcinations, etc [23]. These methods have been widely used for preparing noble metal catalysts on support materials. In 1951, Turkevitch et. al. [24] suggested the use of citrate for reducing $HAuCl_4$ in aqueous conditions to synthesize gold nanoparticles with dimensions of approximately 20 nm. Gold nanoparticles of predetermined dimensions could be obtained by controlling the ratio between the reducing and stabilizing agents [25]. This method still remains very popular and is especially useful for applications where the surface of the gold particles are functionalized or capped with ligands. In yet another approach Zhao and Crooks [26-27] reported the use of dendrimers as templates for the synthesis of nanoparticles. Here, dendrimers act as a template and stabilizer. It can be seen that in general the chemical reduction of metal salts in their liquid phase is the most convenient method to prepare metal nanoparticles [24-28].

From the different methods reported in literature, the one developed by Brust and Schriffin [29-30] for the synthesis of alkanethiolate-protected gold nanoparticles (Au NPs) is still the method of choice due to its simplicity and ease of preparation. In this method, the chloroaurate anion $[AuCl_4]^-$ in the aqueous phase is transferred to an organic phase of toluene using tetraoctylammonium bromide as the phase transfer catalyst and then reduced using an aqueous solution of sodium borohydride in the presence of thiols. The individual gold nanoparticles are stabilized by thiols which form monolayer around it. These nanoparticles can be separated from the solution and redissolved in a variety of organic solvents without significantly affecting their particle size distribution [31]. A large volume of work has been subsequently reported for the synthesis of monolayer protected clusters (MPCs) which are dense

Au NPs, stabilized by variety of functionalized thiol ligands [32-33]. By using polar terminal functional groups in thiols, it is possible to obtain MPCs which can be dispersed in polar solvents like water. These MPCs are finding potential applications in sensors [34], and as photoactive materials [35]. Due to the phenomenon of surface plasmon resonance, they exhibit intense color and their energy levels are quantized due to their small size. By tailoring the terminal functional groups of the ligand, it is possible to attain desired wetting properties. This method can also be used to link enzymes and other biomolecules on the electrode surfaces to exploit the catalytic properties of the nanoparticles and in the development of biosensors [34].

In spite of the considerable progress in the purification method and in obtaining mono dispersed nanoparticles, there are no reports on electrochemical methods of preparation of the thiol capped metal nanoparticles in literature. There are some interesting reports of electrochemical preparations of Au, Ag, Pt and Pd nanoparticles in literature [36-44]. For example Reetz et. al. reported the electrochemical preparation of Pd nanocrystals stabilized by tetraalkylammonium using sacrificial anode [37-39]. They demonstrated that particle size is an inverse function of applied overpotential [37]. Their method represents a refinement of the classical electrorefining process and consists of six elementary steps, which are oxidative dissolution of anode, migration of metal ions to the cathodes, reduction of ions to zero-valent state, formation of particles by nucleation and growth, arrest of growth by capping agents, and precipitation of particles. Recently, Pan et. al. reported the synthesis of Pd nanoparticles by electrochemical reduction of $[PdCl_4]^{2-}$ and studied its voltammetric behavior and electrocatalytic properties [40]. There are also reports of sonoelectrochemical method of synthesis of Au NPs from bulk gold substrates [41].

Here, we show that an electrochemical method can be used for synthesizing the gold nanoparticles using thiols as stabilizers. A gold wire electrode forms the sacrificial anode. The required thiol can be easily dissolved in equal proportion of ethanol-water mixture, which acts as the electrolyte medium. The synthesized thiol capped Au NPs are characterized by UV-vis spectroscopy, FTIR, and TEM.

2.2 Experimental Section

2.2.1 Chemicals

All of the chemical reagents used in this study were analytical grade (AR) reagents. Sodium borohydride (Aldrich), KCl (Merck), Decanethiol (Aldrich), 11-Mercaptoundecanoic acid (Aldrich), Ethanol (Merck), Toluene (Merck), and Millipore Milli-Q water of resistivity 18 MΩ cm were used for all the studies.

2.2.2 Electrode Pretreatment

Two 0.5 mm diameter gold wires of 99.9% purity with an exposed length of about 5mm were used as an anode and a cathode respectively. The electrodes were cleaned in a "piranha" solution, which is a mixture of 30% H_2O_2 and concentrated H_2SO_4 in 1:3 ratio. *(Caution! Piranha solution is very reactive with organic compounds, storing in a closed container and exposure to direct contact should be avoided*). The wire electrode to be used as anode is subjected to potential cycling between – 0.5 V and 1.4 V at a scan rate of 200mV s^{-1} in 0.1M H_2SO_4 for about 20 cycles to effect electrochemical cleaning.

2.2.3 Preparation of the Electrolyte

Mixture of 1% $NaBH_4$, 1M KCl in Millipore water and 20 mM decanethiol in ethanol or 20 mM 11-mercaptoundecanioc acid (MUA) in ethanol in equal volume proportion constitute the electrolyte. We have also synthesized nanoparticles by carrying out the electrochemical dissolution of the gold electrode in the absence of $NaBH_4$.

2.2.4 Electrochemical Studies

The electrochemical dissolution of gold wire electrode was carried out in a standard electrochemical cell of 100 ml capacity at ambient temperature (about 25^0C) using a two electrode configuration. The two electrodes were kept at a distance of about 5 mm and the electrolysis is carried out under magnetic stirring.

2.2.5 Instrumentation

The experiments were conducted at different controlled current densities of 0.1, 0.2, 0.3, 0.4, and 0.5 A cm^{-2} under chronopotentiometry mode using an EG&G potentiostat (Model 263 A).

The characterization of the purified nanoparticles was carried out using UV-vis spectrometer Hitachi U3200, transmission electron microscopy (TEM) FEI (Tecnai G2 20 S-Twin 200kV), and fourier transform infrared (FTIR) spectroscopy Shimadzu 8400.

2.2.6 Purification of DT Protected Au NPs

The Au NPs synthesized using decanethiol floats on top of the electrolyte, as these NPs are hydrophobic. These particles were extracted into the toluene, later removed under vacuum, and finally washed several times with alcohol to remove excess of decanethiol. The particles were dried in air. The purified decanethiol capped nanoparticles were dispersed in toluene used for characterization.

2.2.7 Purification of MUA Protected Au NPs

The Au NPs synthesized using MUA are water soluble and hence the particles get dispersed in the electrolyte medium during the electrolysis. After the electrolysis was completed the NPs were centrifuged and washed with ethanol and with water. The MUA protected nanoparticles were redissolved in water for characterization.

2.3 Results and Discussions

2.3.1 Electrochemical Synthesis of Decanethiol Stabilized Au NPs

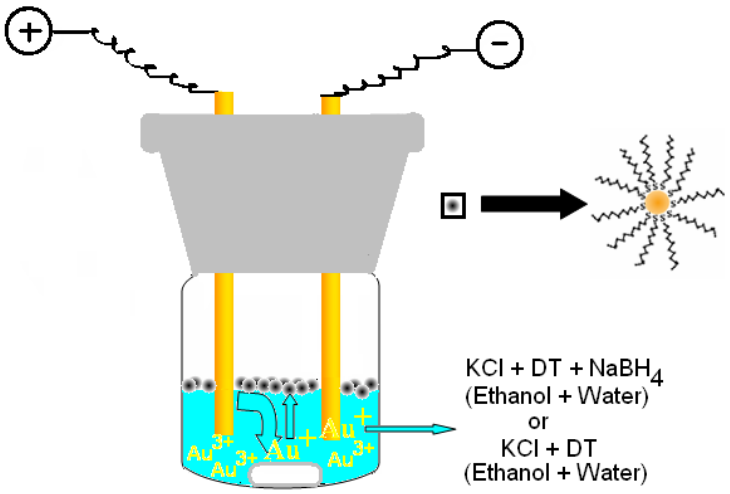

Figure 1. Schematic representation of the electrochemical setup used for the synthesis of nanaoparticles.

Electrochemical synthesis of Au NPs was carried out using two gold wire electrodes in chronopotentiometric mode. The electrolyte contains mixture of KCl as a supporting electrolyte in water and thiol in ethanol as a stabilizer in equal volume. During the electrolysis, there is a profuse evolution of O_2 at the anode with the simultaneous dissolution of the metal. The black particles float on the electrolyte solution within about 5 minutes of electrolysis at a current density of 0.5 A cm^{-2}, where decanethiol act as a stabilizer. The electrolysis was continued for about 30 minutes. After this, the floating particles in the aqueous suspension were extracted into toluene to obtain a clear brownish dispersion. The solvent was removed from the nanoparticles under vacuum, purified by washing with ethanol repeatedly to remove excess thiol and dried under vacuum. The nanoparticles can be redispersed in organic solvents several times. Figure 1 shows the schematic representation of the experimental setup used for the electrochemical synthesis of nanoparticles. Figure 2 shows the photograph of purified well dispersed nanoparticles in toluene.

Figure 2. Shows the photograph of decanethiol stabilized gold nanoparticles dispersion in toluene.

2.3.1.1 UV-vis Studies

Surface plasmon resonance band of gold nanoparticles in toluene solution was observed using UV-vis spectrophotometer. Figure 3 shows the representative UV-vis spectrum of Au NPs synthesized at a current density of 0.5 A cm^{-2} that shows an absorption peak around 522nm, which is characteristic of the surface plasmon resonance (SPR) band of Au NPs. We find that there is only small variation in the wavelength maximum for the nanoparticles prepared under varying current densities from 0.1 to 0.5 A cm^{-2}. We have optimized the current density of 0.5 A cm^{-2} for the Au NP synthesis. The SPR band remains the same as that of the freshly prepared

sample even after drying and redissolving in toluene several times. This clearly shows the formation of very stable nanoparticles. Figure 4 shows the UV-vis spectrum of Au NPs synthesized under identical conditions, but without the addition of $NaBH_4$. The spectrum shows a broad absorption band around 526 nm. This indicates the wide size distribution of NPs synthesized in the absence of $NaBH_4$ compared to the NPs synthesized in the presence of $NaBH_4$.

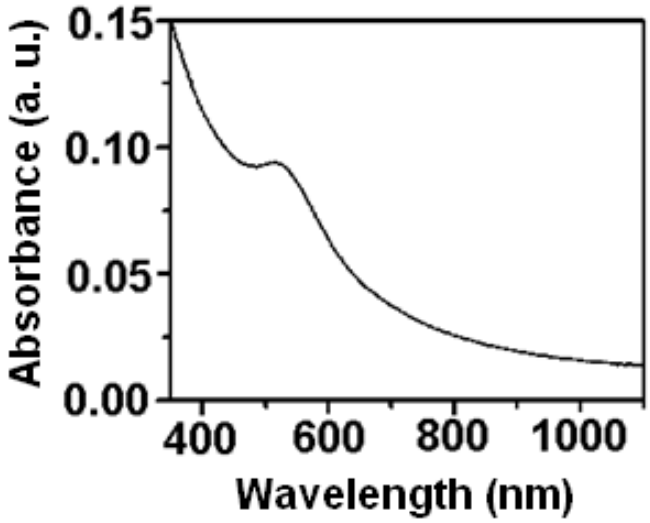

Figure 3. UV-vis spectrogram of the Au NPs dissolved in toluene synthesized using KCl, DT and $NaBH_4$ at a current density of 0.5 A cm^{-2}.

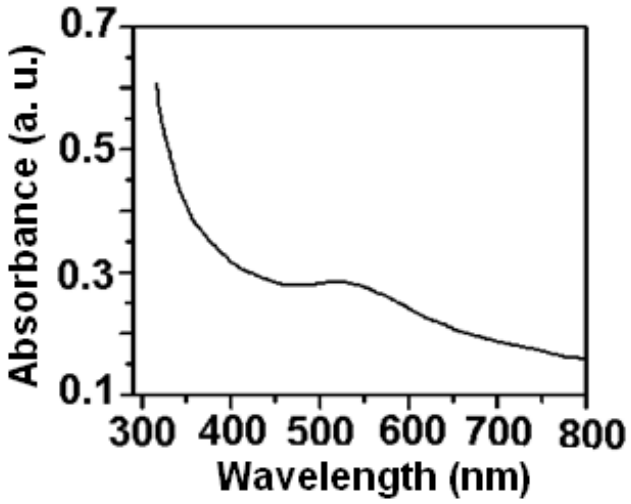

Figure 4. UV-vis spectrogram of the Au NPs taken in toluene synthesized using KCl and DT (in absence of $NaBH_4$) at a current density of 0.5 A cm^{-2}.

2.3.1.2 TEM Studies

Figure 5 shows the transmission electron microscopy (TEM) image of the gold nanoparticles stabilized with decanethiol under different magnifications. The figure 5b is the high resolution TEM image of 5a. The histogram of the particle size distribution of Figure 5b is shown in the figure 6. The sizes of the majority of the particles are between 1 – 3 nm and are well dispersed without aggregation. The selected area diffraction pattern of Au NPs shown in Figure 7 exhibits diffusive rings which is typical of nanometer size particles. The characteristic rings in the polycrystalline diffraction pattern can be indexed as shown in the Table 1. Figure 8 shows the HRTEM image of a single Au NP showing the lattice fringes. The most frequently observed lattice fringes in the high-resolution image are 0.23 nm and 0.2 nm which can be indexed respectively to the lattice spacing of (111) and (200) fcc structure of gold. Interestingly, we could also synthesize NPs in the absence of $NaBH_4$. Figure 9 shows the TEM image of Au NPs synthesized without using $NaBH_4$. The sizes of the particles are in the range of 4-13 nm. The size distribution of particles is wider compared to the NPs synthesized using $NaBH_4$. Figure 10 shows the selected area diffraction pattern. The characteristic rings in the polycrystalline diffraction pattern can be indexed as shown in the Table 2.

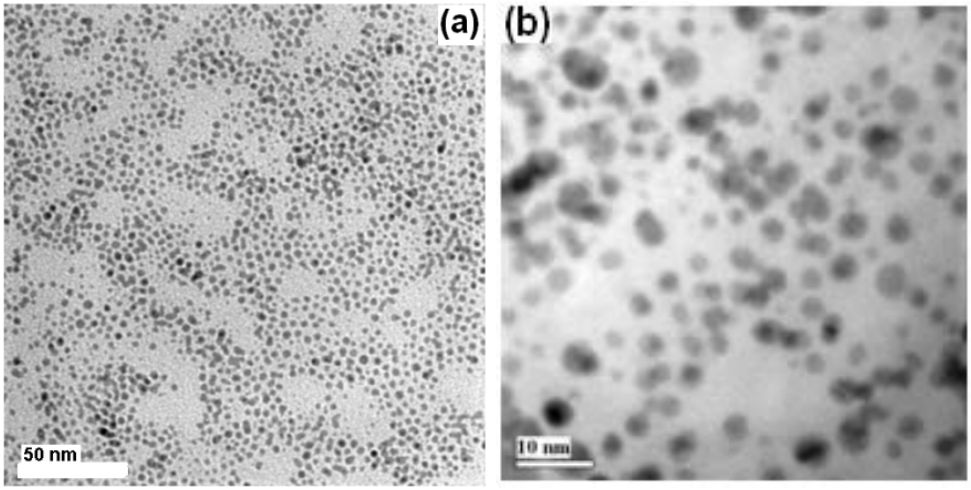

Figure 5. (a) TEM image of electrochemically synthesized gold nanoparticles using KCl, DT, and $NaBH_4$, (b) TEM image under higher magnification.

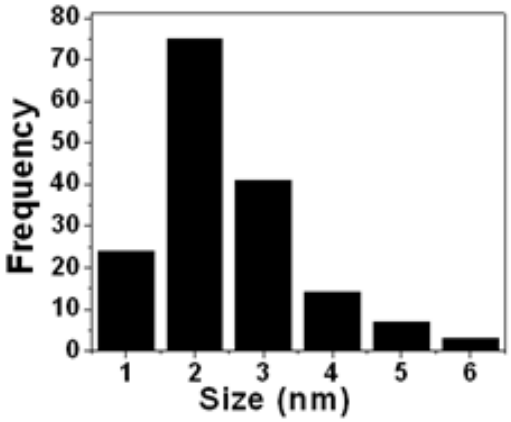

Figure 6. Histogram for the size distribution of Au NPs synthesized using KCl, DT, and $NaBH_4$.

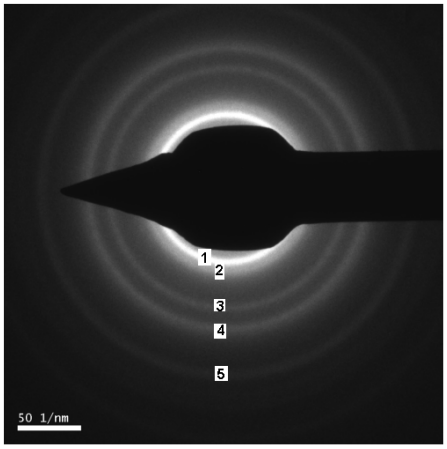

Figure 7. Selected are diffraction pattern of the Au NPs synthesized using KCl, DT, and $NaBH_4$.

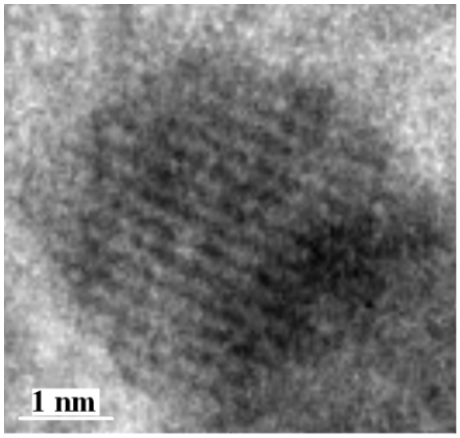

Figure 8. High resolution TEM image of Au NP synthesized using KCl, DT and $NaBH_4$ showing the lattice fringes.

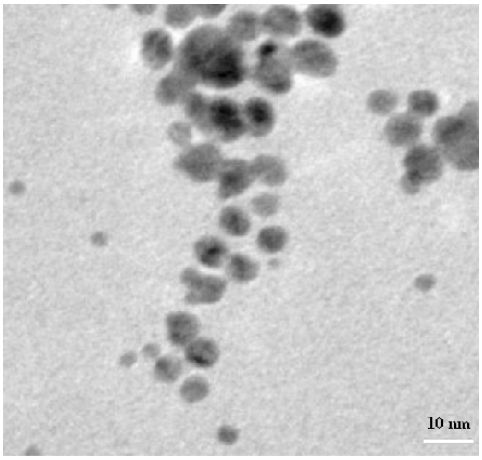

Figure 9. TEM image of electrochemically synthesized gold nanoparticles using KCl and DT (in the absence of $NaBH_4$).

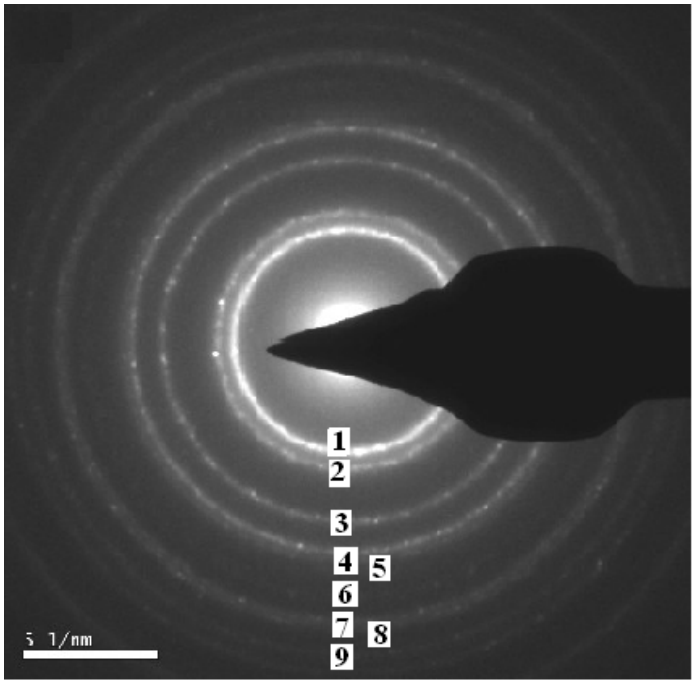

Figure 10. Selected area diffraction pattern of the Au NPs synthesized electrochemically using KCl and DT.

Sl. No.	KCl, DT, and $NaBH_4$	
	Index	d-Spacing
1	(111)	2.36
2	(200)	2.03
3	(220)	1.45
4	(311)	1.22
5	(331)	0.93

Table 1. Indexing of electron diffraction pattern for the electrochemically synthesized gold nanoparticles.

Sl. No.	KCl and DT (Without $NaBH_4$)	
	d-Spacing	Index
1	2.35	(111)
2	2.02	(200)
3	1.43	(220)
4	1.22	(311)
5	1.17	(222)
6	1.02	(400)
7	0.93	(331)
8	0.92	(420)
9	0.84	(422)

Table 2. Indexing of electron diffraction pattern for the electrochemically synthesized gold nanoparticles.

2.3.1.3 Mechanism of NPs Formation

The mechanism of nanoparticles formation by electrochemical method can be explained as follows: Reetz *et al*. had shown the electrochemical synthesis of Pd nanoparticles, the charged species Pd_n^{m+} is formed at the anode, which migrates and discharge at the cathode to form Pd^0 clusters that are subsequently associated and stabilized by tetraalkylammonium salts in the solution [37].

It was shown earlier that the gold electrode dissolves in electrolyte medium, viz, aqueous chloride as monovalent $[AuCl_2]^-$ and predominantly as trivalent $[AuCl_4]^-$ complexes [44]. It was proposed that $[AuCl_2]^-$ forms polymeric thiolated complex in the presence of organic thiol, which acts as a chelating ligand [45-48]. $NaBH_4$ reduces the gold chloride complexes to Au clusters which are subsequently stabilized by thiol. In the absence of $NaBH_4$, ethanol in the electrolyte acts as a reducing agent though the process of formation is relatively slow.

2.3.2 Electrochemical Synthesis of Au NPs using Functionalized Thiol 11-Mercaptoundecanoic Acid (MUA)

To obtain the functionalized Au NPs, we have synthesized electrochemically Au NPs in the presence of MUA using KCl as a supporting electrolyte. The MUA protected Au NPs were synthesized in the presence of $NaBH_4$ and also in its absence. In the later case ethanol present in the electrolyte acts as a reducing agent. The experiments were conducted at constant anodic current density of 0.5 A cm^{-2} for 30 minutes duration. During the electrochemical dissolution of gold, the electrolysis of water and evolution of gases on both the electrodes take place as a parallel reaction (*Caution! Use a cell with opening near both the electrodes to allow the gases to escape*). Simultaneously, the gold wire starts dissolving and the electrolyte turns red within a few minutes of electrolysis indicating the formation of Au NPs in the solution. Electrolysis was continued for 30 minutes. The NPs were dispersed during the synthesis, as MUA stabilized NPs are water soluble, unlike decanethiol stabilized NPs where, the NPs float on top of the electrolyte. Figure 11a shows the photographs of Au NPs formed in the electrolyte which are purified and redissolved in water. These nanoparticles in the solution phase aggregate and precipitate after about 8 hour of purification in water as shown in the Figure 11b. Due to the aggregation, these NPs change its color from red to the black color. The aggregated nanoparticles are not soluble in water. However, the purified and dried nanoparticles are quite stable for more than 6 months.

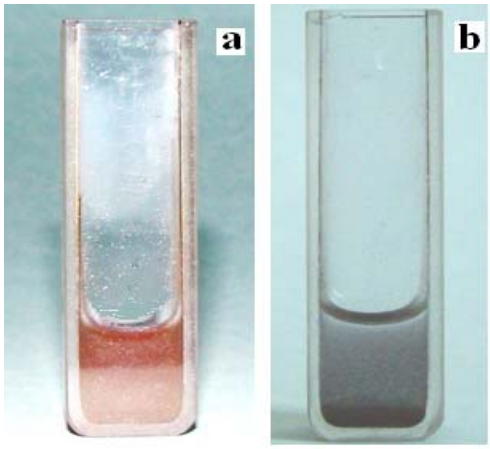

Figure 11. Shows the photographs of Au NPs formed in the electrolyte during the synthesis: (a) purified Au NPs in water and (b) 8 hour after purification in water.

2.3.2.1 UV-vis Studies

The UV-vis spectrum of the purified NPs synthesized using KCl, MUA, and $NaBH_4$ shown in Figure 12 has a peak at 535 nm, which is a characteristic surface plasmon band of Au NPs. Figure 13 shows the UV-vis spectrum of particles synthesized using KCl and MUA. The spectrum shows a peak at 535 nm, indicating the formation of NPs in the solution. The NPs formation in the absence of $NaBH_4$ is due to the ethanol present in the electrolyte, which acts as a reducing agent. Purified NPs which are kept in the solid state for more than 6 months at room temperature. The UV-vis spectrum was taken after dissolving Au NPs in water. The surface Plasmon band remains same as freshly prepared nanoparticles which show that the NPs are stable in the solid state.

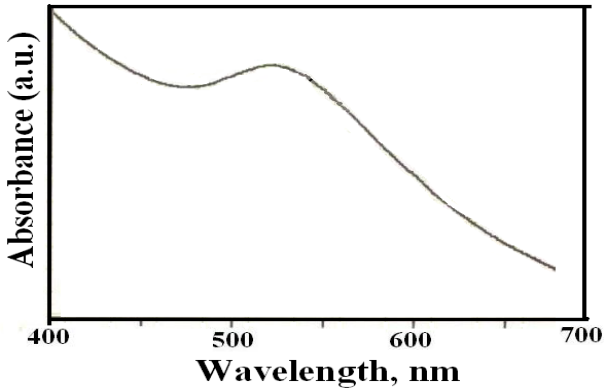

Figure 12. UV-visible spectrum of MUA stabilized Au NPs synthesized using KCl, MUA and $NaBH_4$ at a current density of 0.5 A cm^{-2}.

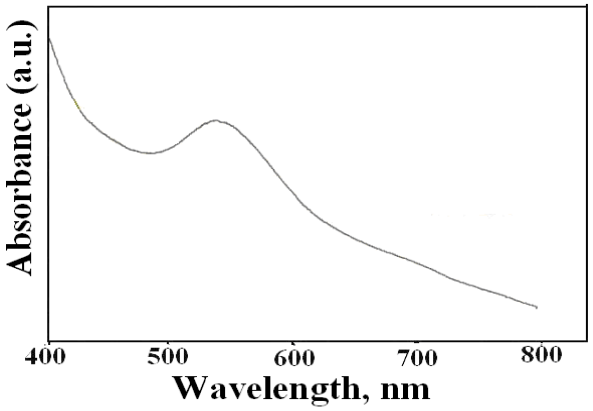

Figure 13. UV-visible spectrum of MUA stabilized Au NPs synthesized using KCl and MUA at a current density of 0.5 A cm^{-2}.

2.3.2.2 Fourier Transform Infrared Spectroscopy (FTIR) Studies

The purified solution of MUA stabilized Au NPs was characterized by IR using KBr pellet. Figure 14 shows the IR spectrum of purified MUA stabilized Au NPs. The spectrum shows υ_{O-H} strectching bond superimposed on the aliphatic C-H stretch vibration around 3000 cm^{-1}, υ_{C-H} saturated vibration stretching at 2800-3100 cm^{-1}, $\upsilon_{C=O}$ as peak at 1708 cm^{-1}. The finger print region of IR shows the band at 1461cm^{-1}, 1290 cm^{-1}, which corresponds to the interacting υ_{C-O} stretch and in-plane υ_{C-O-H} deformation vibration. The band corresponding to the υ_{S-H} stretching vibration at 2554 cm^{-1} is absent for the Au-MUA showing that the MUA is bound on the gold nanoparticles through sulfur atom.

2.3.2.3 TEM Studies

Figure 15 shows the transmission electron microscopy (TEM) image of the gold nanoparticles stabilized with MUA under different magnifications. The image shows the very small individual nanoparticles and there are some aggregations of particles as well. The histogram of the particle size distribution of figure 15b is shown in Figure 16. The sizes of the majority of the particles are between 2 – 5 nm and are well dispersed without aggregation.

Figure 17 shows the selected area diffraction pattern of Au NPs. The electron diffraction pattern shows the diffusive rings. The characteristic rings in the polycrystalline diffraction pattern can be indexed and shown in Table 3.

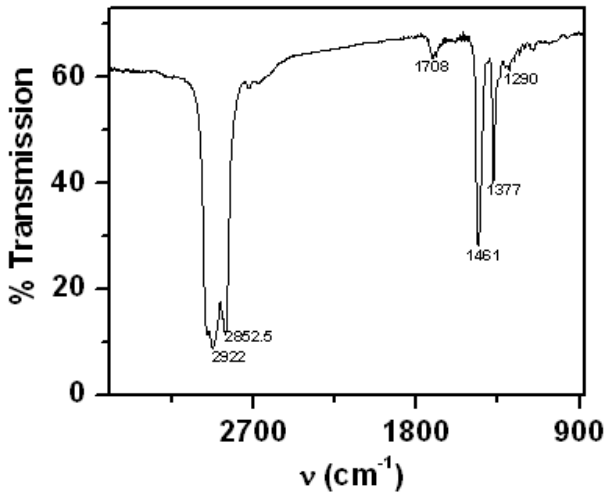

Figure 14. IR spectra of solid particles of MUA stabilized Au NPs synthesized using KCl and MUA (IR spectra was taken using KBr pellet).

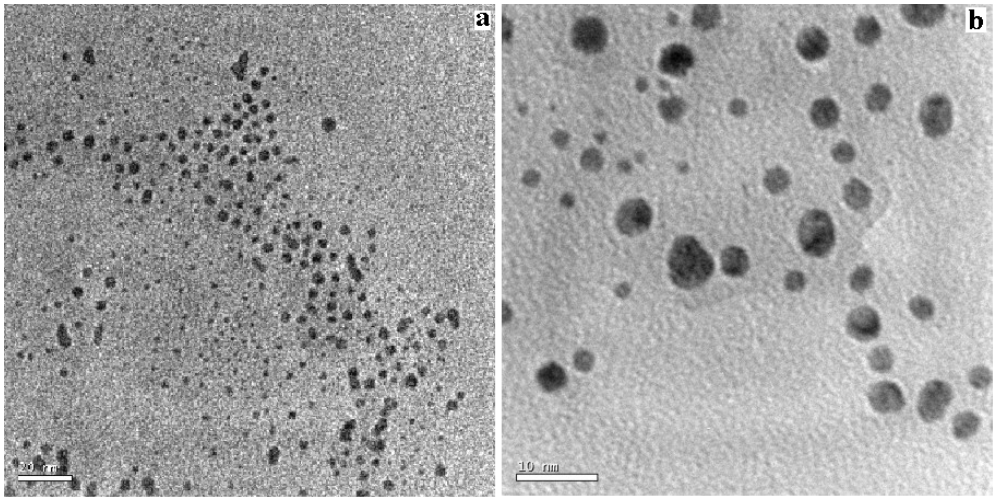

Figure 15. (a) Shows the TEM images of Au NPs synthesized using KCl, MUA, and $NaBH_4$. (Scale bar Shown is 20 nm) (b) The high resolution image (Scale bar Shown is 10 nm).

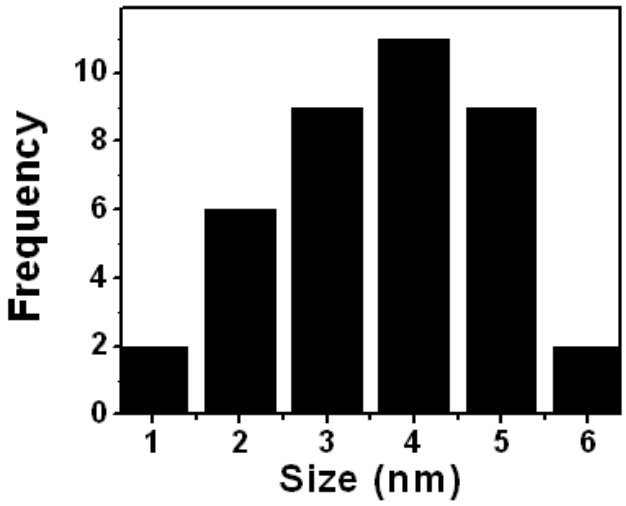

Figure 16. Histogram for the size distribution of Au NPs synthesized electrochemically using KCl, MUA, and $NaBH_4$.

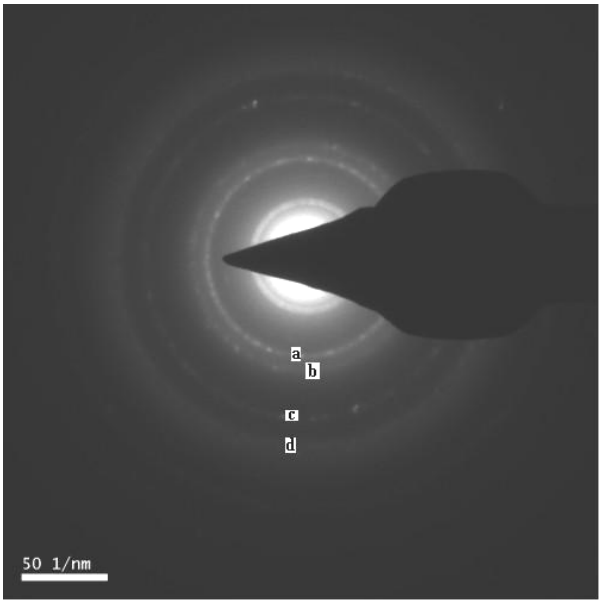

Figure 17. Selected area diffraction pattern of NPs synthesized using KCl, MUA, and $NaBH_4$.

S. No.	KCl, DT, and $NaBH_4$	
	Index	d-Spacing
1	(111)	2.37
2	(200)	2.07
3	(220)	1.46
4	(311)	1.25

Table 3. Indexing of electron diffraction pattern for the electrochemically synthesized Au NPs.

2.4 Conclusions

We have synthesized the thiol stabilized gold nanoparticles (Au NPs) for the first time by the process of electrochemical dissolution of gold. The Au NPs can be synthesized by this method both with and without $NaBH_4$ with KCl as a supporting electrolyte. Here, we have synthesized the gold nanoparticles using the alkanethiol such as DT and functionalized thiol such as MUA. The thiol capped Au NPs were characterized by UV-vis, FTIR, and TEM studies. This method with suitable parametric control has the potential to prepare thiol stabilized Pt, Ag, Cu, etc., nanoparticles. The method presented in this chapter not only produces the thiol stabilized nanoparticles in solution, but also results in the deposition of the nanoparticles on the gold cathode substrate. The next and the following chapters describe the method of formation of thin film of gold constituted of Au nanoparticles and its potential application as high surface area material.

2.5 References

[1] Y. Sun, Y. Xia, *Science* **2002**, *298*, 2176.

[2] N. R. Jana, L. Gearheart, C. J. Murphy, *Chem. Commun.* **2001**, *7*, 617.

[3] J. L. Yao, G. P. Pan, K. H. Xue, D. Y. Wu, B. Ren, D. M. Sun, J. Tang, X. Xu, Z. Q. Tian, *Pure. Appl. Chem.* **2000**, *72*, 221.

[4] J. T. Hu, T. W. Odom, C. M. Lieber, *Acc. Chem. Res.* **1999**, *32*, 435.

[5] J. Wang, G. Liu, A. Merkovi, *J. Am. Chem. Soc.* **2003**, *125*, 3214.

[6] W. P. McConnell, J. P. Novak, L. C. Brousseau, R. R. Fuierer, R. C. Tenent, D. L. Feldheim, *J. Phys. Chem. B* **2000**, *104*, 8925.

[7] K. Ghosh, S. N. Maiti, *J. Appl. Polym. Sci.* **1996**, *60*, 323.

[8] P. R. Andres, J. D. Bielefeld, J. I. Henderson, D. B. Janes, V. R. Kolagunta, C. P. Kubiak, W. Mahoney, R. G. Osifchin, R. Reifenberger, *Science* **1996**, *273*, 1960.

[9] C. B. Murray, S. Sun, H. Doyle, T. Betley, *Mater. Res. Soc. Bull.* **2001**, *26*, 985.

[10] S. Forster, M. Antonietti, *Adv. Mater.* **1998**, *10*, 195.

[11] S. Bharathi, M. Nogami, *Analyst*, **2001**, *126*, 1919.

[12] S. Zhao, S. Chen, S. Wang, D. Li, H. Ma, *Langmuir* **2002**, *18*, 3315.

[13] N. R. Jana, Z. L. Wang, T. Pal, *Langmuir* **2000**, *16*, 2457.

[14] R. S. Ingram, M. J. Hostetler, R. W. Murray, T. G. Schaaff, J. T. Khoury, R. L. Whetten, T. P. Bigioni, D. K. Guthrie, P. N. First, *J. Am. Chem. Soc.* **1997**, *119*, 9279.

[15] S. Chen, R. W. Murray, *J. Phys. Chem. B* **1998**, *102*, 9898.

[16] J. F. Hicks, A. C. Templeton, S. Chen, K. M. Sheran, R. Jasti, R. W. Murray, *Anal. Chem.* **1999**, *71*, 3703.

[17] J. F. Hicks, A. C. Templeton, S. Chen, K. M. Sheran, R. Jasti, R. W. Murray, *J. Am. Chem. Soc.* **1999**, *121*, 5565.

[18] S. Chen, R. W. Murray, *J. Phys. Chem. B* **1999**, *103*, 9996.

[19] T. S. Ahmadi, Z. L. Wang, T. C. Green, A. Henglein, M. A. El Sayed, *Science* **1996**, *272,* 1924.

[20] M. C. Daniel, D. Astruc, *Chem.l Rev.* **2004**, *104*, 293.

[21] G. Schmid, *Chem. Rev.* **1992**, *92*, 1709.

[22] M. Brust, C. J. Kiely, *Colloids and Surfaces A-Physicochemical and Engineering Aspects* **2002**, *202*, 175.

[23] V. Rotello *Nanoparticles Building blocks for nanotechnology,* Springer **2004**,

[24] J. Turkevich, P. C. Stevenson, J. Hillier, *Discussions of the Faraday Society* **1951**, *11*, 55.

[25] K. K. Zadeh, B. Fry, *Nanotechnology Enabled Sensors*, Springer **2008**

[26] M. Q. Zhao, R. M. Crooks, *Adv. Mater.* **1999**, *11*, 217.

[27] R. M. Crooks, M. Q. Zhao, L. Sun, V. Chechik, L. K. Yeung, *Accounts of Chemical Research* **2001,** *34*, 181.

[28] C. K. Tan, V. Newberry, T. R. Webb, C. A. McAuliffe, *J. Chem. Soc. Dalton Trans.* **1987**, 1299.

[29] M. Brust, M. Walker, D. Bethell. D. J. Schiffrin, R. Whyman, *J. Chem. Soc., Chem. Commun.* **1994**, 801.

[30] M. Brust, J. Fink, D. Bethell, D. J. Schiffrin, C. J. Kiely, *J. Chem. Soc., Chem. Commun*. **1995**, 1655.

[31] C. A. Walters, A. J. Mills, K. A. Johnson, D. J. Schriffin, *Chem. Commun.* **2003**, 540.

[32] S. Chen, *Langmuir* **1999**, *15,* 7551.

[33] S. Chen, R. W. Murray, *Langmuir* **1999**, *15,* 682.

[34] Y. Xiao, F. Patolsky, E. Katz, J. F. Hainfeld, I. Willner, *Science* **2003**, *299*, 1877.

[35] N. Chandrasekharan, P. V. Kamat, *J. Phys. Chem. B,* **2000**, *104,* 10851.

[36] C. N. R. Rao, P. J. Thomas, G. U. Kulkarni, *Nanocrystal, Synthesis, Properties and Applications*, Springer **2007**

[37] M. T. Reetz, W. Helbig, *J. Am. Chem. Soc.* **1994**, *116,* 7401.

[38] R. Breinbauer, T. T. Albrecht, W. Vogel, *Chem. Eur*. *J.* **2001**, *7,* 1084.

[39] M. T. Reetz, W. Helbig, S. A. Quaiser, U. Stimming, N. Breuer, R. Vogel *Science* **1995**, *267*, 367.

[40] W. Pan, X. Zhang, H. Ma, J. Zhang, *J. Phys. Chem. C* **2008**, *112*, 2456.

[41] Y. C. Liu, L. H. Lin, W. H. Chiu, *J. Phys. Chem. B* **2004**, *108*, 19237.

[42] S. Huang, H. Ma, X. Zhang, F. Yong, X. Feng, W. Pan, X. Wang, Y. Wang, S. Chen, *J. Phys. Chem. B* **2005**, *109,* 19823.

[43] Y. Y. Yu, S. S. Chang, C. L. Lee, C. R. C. Wang *J. Phys. Chem. B* **1997**, *101,* 6661.

[44] B. S. Yin, H. Y. Ma, S. Y. Wang, S. H. Chen, J. *Phys. Chem. B* **2003**, *107*, 8898.

[45] J. H. Gallego, C. E. Castellano, A. J. Calandra, A. J. Arvia, *J. Electroanal. Chem.* **1975**, *66*, 207.

[46] R. P. Brias, M. Hu, L. Qian, E. S. Lymar, J. F. Hainfeld, *J. Am. Chem. Soc.* **2008**, *130*, 975.
[47] T. G. Schaaff, M. N. Shafigullin, J. T. Khoury, I. Vezmar, R. L. Whetten, W. G. Cullen, P. N. First, C. Gutirrez-Wing, J. Ascensio, M. J. Jose-Yacamn, *J. Phys. Chem. B* **1997**, *101*, 7885.
[48] B. Wenzel, P. Lonnecke, E. Hey-Hawkins, *Eur. J. Inorg. Chem.* **2002**, 1761.